

Conditional Prototype Rectification Prompt Learning

Haoxing Chen¹, Yaohui Li², Zizheng Huang^{1,2}, Yan Hong¹, Zhuoer Xu¹
Zhangxuan Gu¹, Jun Lan¹, Huijia Zhu¹, Weiqiang Wang¹
Tiansuan Lab, Ant Group¹, Nanjing University²
hx.chen@hotmail.com, yaohuili@smail.nju.edu.cn

Abstract

Pre-trained large-scale vision-language models (VLMs) have acquired profound understanding of general visual concepts. Recent advancements in efficient transfer learning (ETL) have shown remarkable success in fine-tuning VLMs within the scenario of limited data, introducing only a few parameters to harness task-specific insights from VLMs. Despite significant progress, current leading ETL methods tend to overfit the narrow distributions of base classes seen during training and encounter two primary challenges: (i) only utilizing uni-modal information to modeling task-specific knowledge; and (ii) using costly and time-consuming methods to supplement knowledge. To address these issues, we propose a Conditional Prototype Rectification Prompt Learning (CPR) method to correct the bias of base examples and augment limited data in an effective way. Specifically, we alleviate overfitting on base classes from two aspects. First, each input image acquires knowledge from both textual and visual prototypes, and then generates sample-conditional text tokens. Second, we extract utilizable knowledge from unlabeled data to further refine the prototypes. These two strategies mitigate biases stemming from base classes, yielding a more effective classifier. Extensive experiments on 11 benchmark datasets show that our CPR achieves state-of-the-art performance on both few-shot classification and base-to-new generalization tasks. Our code is available at <https://github.com/chenhaoxing/CPR>.

1. Introduction

Leveraging the vast array of image-text association pairs, the trained visual-language models (VLMs) embody critical general knowledge, thereby exhibiting enhanced generalizability across diverse tasks. In recent developments, several visual-language models like Contrastive Language-Image Pre-training [19] (CLIP), Flamingo [1], and ALIGN [12] have been introduced. While VLMs are proficient at extracting visual and textual descriptions, their training ne-

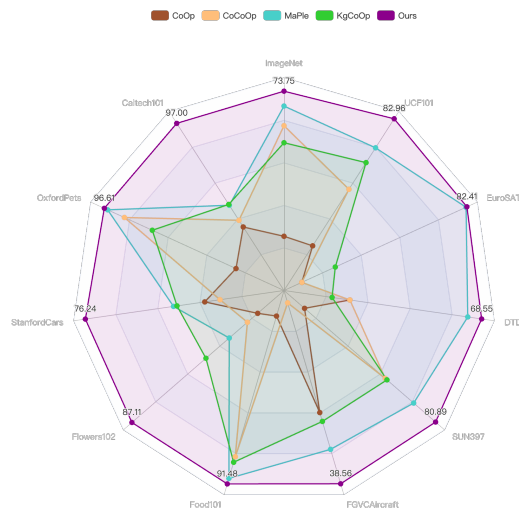


Figure 1. Comparison of different efficient transfer learning methods on base-to-new generalization task.

cessitates extensive, high-quality datasets. Nevertheless, amassing substantial data for training task-specific models in real-world visual-language applications poses a challenge. To circumvent this issue, efficient transfer learning (ETL) methods [15, 26, 29, 30, 32] have been devised to fine-tune pre-trained VLMs for downstream tasks, demonstrating remarkable efficacy in various few-shot or zero-shot visual recognition tasks.

There are two notable ETL methods for VLMs: prompt tuning [26, 29–31] and adapter-style tuning [9, 15, 32]. Prompt tuning modifies the textual classifier by incorporating learnable prompts at the input, significantly outperforming zero-shot CLIP with few-shot examples, seen in CoOp [30] and CoCoOp [29]. Conversely, adapter-style tuning adjusts textual classifiers or visual features at the output, using the textual encoder just once. For example, CLIP-Adapter [9] employs a bottleneck layer to fine-tune embeddings, surpassing zero-shot CLIP by 3.02% on ImageNet in a one-shot scenario. TaskRes [27] adjusts textual

embeddings with task-specific parameters, acting as independent residuals. Another approach enhances downstream task knowledge using large scale databases or generative models, like Sus-X [23] and C2A [21].

However, two main limitations exist in current ETL research: 1) Many approaches, like CLIP-Adapter [9] and TaskRes [27], focus on task-specific knowledge from only one modality, relying solely on visual or textual features for adaptation. 2) Using generative models or large scale datasets to augment datasets typically requires substantial computational resources, impacting efficiency. In low-data scenarios, limited samples struggle to adequately reveal structural knowledge for downstream tasks, potentially biasing the model toward certain attributes like color or shape. This can limit transferability and generalization. Therefore, integrating multi-modality knowledge and discovering efficient strategies to enrich the dataset are essential for VLM tuning, addressing the biases that stem from data scarcity.

To alleviate these limitations, we propose two prototype rectification strategies, referred to as conditional prototype rectification learning, which aim to model task-specific knowledge for downstream tasks by integrating textual and visual structural knowledge as well as knowledge from unlabeled samples. To tackle the first limitation, we introduce the Conditional Adapter (CoAdapter), which leverages the input image alongside visual and textual prototypes to capture structured knowledge pertinent to downstream tasks, producing sample-specific prototypes. This equips the feature adapter with a comprehensive and accurate understanding essential for these tasks. Addressing the second limitation, we devise the Nearest Neighbor Rectification (NNR) strategy. It identifies the k nearest samples from the unlabeled dataset that align with the prototypes generated by the CoAdapter, facilitating rectification. This process effectively utilizes the latent knowledge within the unlabeled samples, enriching the learning context of model. As shown in Figure 1, CPR achieves significant improvements over the previous state-of-the-art algorithms on both few-shot classification and base-to-new generalization tasks.

The contributions of this paper are summarized as follows:

- We propose conditional prototype rectification learning (CPR), which introduce two prototype rectification strategies designed to amend the bias inherited from base examples and effectively augment limited data.
- We introduce a novel adapter-style tuning approach, the Conditional Adapter (CoAdapter), for efficiently transfer learning (ETL) of vision-language models (VLMs). This strategy harnesses dual-modality structure knowledge from both textual and visual domains, allowing the feature adapter to utilize integrated visual and textual insights. This fusion facilitates enhanced learning of task-specific knowledge from downstream tasks, leading to ef-

fective VLM tuning.

- we propose the Nearest Neighbor Rectification (NNR), a method of knowledge completion that addresses the issue of biased knowledge without the need for auxiliary or synthetic data. NNR capitalizes on the concept of nearest neighbors to extract valuable insights from test samples, enriching the information available from a few shots.
- We evaluate our CPR across 11 popular benchmarks in both few-shot classification and base-to-new generalization settings. The evaluations reveal that CPR markedly surpasses earlier prompt-based and adapter-style methodologies, showcasing notable efficacy even in demanding fine-grained image classification tasks, exemplified by FGVC Aircraft.

2. Related Works

2.1. Visual-Language Pre-training

The principal aim of Visual-Language Pre-training (VLP) is to execute multimodal pre-training employing extensive datasets comprising image-text pairs, aiming to develop universal representations for text and images. This approach is intended to improve the effectiveness of model in various downstream tasks. These tasks notably include zero-shot learning, few-shot classification, cross-modal generation, open-world segmentation, and open-world detection, among others. In this context, models such as VisualBERT, OSCAR, and Uniter use BERT to process raw text, achieving significant results in multimodal tasks like Visual Question Answering (VQA), which demonstrates their substantial application potential. These successes emphasize the importance of well-designed fusion encoders in merging cross-modal interactions. Additionally, recent studies like CLIP, DeCLIP, and ALIGN have demonstrated the effectiveness of visual-language contrastive learning in producing features that are useful for downstream tasks. These features are acquired by simply calculating the dot product between visual and linguistic embeddings, offering a straightforward understanding of multimodal interactions. Moreover, these approaches avoid the need for self-attention or cross-attention mechanisms, allowing for the precomputation and storage of multimodal embeddings without the need for further modifications, thus increasing efficiency and easing their integration into other tasks.

2.2. Efficient Transfer Learning

The objective of Efficient Transfer Learning (ETL) is to facilitate the transfer of specific task knowledge to downstream tasks by adjusting selected parameters in pre-trained visual-language models (VLMs). ETL can primarily be categorized into two methods: prompt tuning and adapter-style tuning.

Prompt tuning originates from the field of Natural Lan-

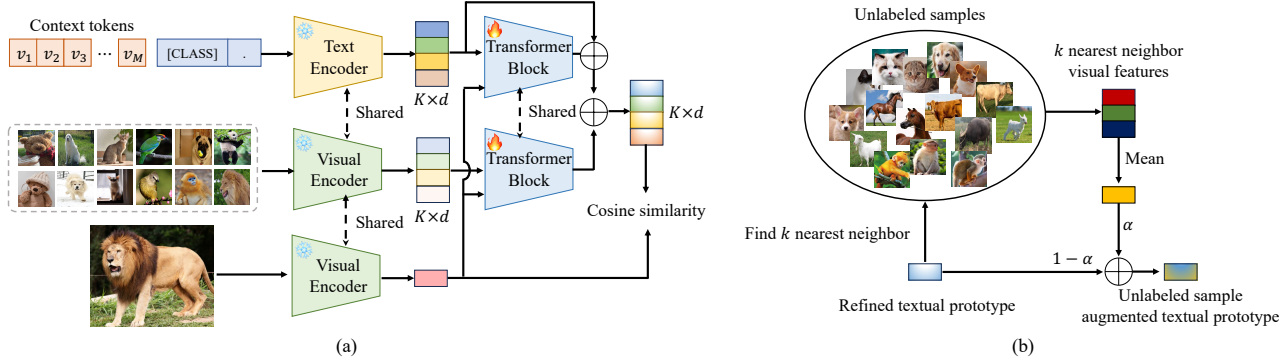


Figure 2. Our approach, Conditional Prototype Rectification Prompt Learning (CPR), includes two strategies: (a) Conditional Adapter exploits connections between input images and both visual and textual prototypes, integrating textual and visual structures to model task-specific knowledge. (b) Nearest Neighbor Rectification leverages unlabeled data to avoid external or synthetic data, addressing biases and limitations in few-shot learning.

guage Processing (NLP) and is designed to apply differentiated prompt templates for various NLP tasks. To adapt pre-trained VLMs to downstream tasks, the prompt tuning method introduces the use of task-related textual tokens to infer specific textual knowledge for the task. For instance, in the CLIP model, a manually crafted template “a photo of a [CLASS]” is employed to construct text embeddings for zero-shot prediction, enhancing performance by 1.9% on the ImageNet dataset compared to the linear probing technique. However, these manually defined prompts have limited capability in describing downstream tasks, overlooking the specific knowledge of the current task. To address this issue, Context Optimization (CoOp) introduces learnable soft prompts derived from few-shot annotated examples instead of fixed manual prompts. The limitation of CoOp lies in that it generates a unique and fixed learnable prompt for images in each task, neglecting the variation in image features. Consequently, Conditional Context Optimization (CoCoOp) was developed to generate image-specific contextual prompts, which are combined with textual context for prompt tuning. Specifically, CoCoOp utilizes a lightweight neural network to create a learnable text prompt vector. To acquire tokens highly relevant to the task, ProDA introduces the learning of a prior distribution for prompts. Moreover, ProGrad selectively updates only those prompt gradients that align with the “general knowledge” generated from the original prompts.

Distinct from prompt tuning, the adapter-style approach modulates textual and visual features to adapt VLMs to downstream tasks. In early work, CLIP-Adapter employed a bottleneck layer to enhance few-shot classification performance. TaskRes [27] introduced a task-independent adapter aimed at decoupling the prior knowledge of pre-trained model from task-specific knowledge. Furthermore, some studies explored acquiring additional prior knowledge from

other large pre-trained models, such as DINO, which also showed promising results in the context of adapter-style applications.

In existing methodologies, the works most relevant to our study are CoCoOp and Sus-X. CoCoOp can be regarded as the baseline model for our proposed CPR. Unlike CoCoOp, our CPR considers not only the input image itself but also the structural relationship between the input image and both visual and textual prototypes to further enhance the performance of learnable prompts. Sus-X introduces a text-image generative model to augment the original support set, whereas CPR utilizes unlabeled samples from the test set for prototype refinement, offering greater efficiency.

3. Preliminaries

We first provide brief reviews on the adopted VLM, i.e., contrastive language-image pre-training (CLIP) [19], recap two mainstream approaches for ETL on VLMs, i.e., prompt tuning and adapter-style tuning.

3.1. Contrastive Language-Image Pre-training

Contrastive Language-Image Pre-training (CLIP) [19] aims to acquire visual representations through natural language supervision. CLIP consists of two encoders: one for images and another for text. The image encoder can be either ResNet [10] or Vision Transformer [7] (ViT), transforming images into feature vectors. The text encoder is a Transformer [24] that takes a sequence of word tokens as input and produces a vectorized representation.

CLIP is trained using 400 million image-text pairs and employs a contrastive loss to learn a joint embedding space for both modalities, enabling CLIP to effectively capture a wide range of visual concepts and learn universal visual representations. Specifically, for an input image x belonging to one of the classes $Y = \{y_1, y_2, \dots, y_C\}$, the image

encoder ϕ extracts image features $z = f(x) \in \mathbb{R}^d$. To obtain the corresponding text features $w_i \in \{1, \dots, C\}$, names of all given classes are filled into the fixed prompt template "a photo of a [CLASS]" (e.g., bear, urocissa erythrorhyncha), generating text descriptions A , which are then further encoded into text embeddings $W = g(A) \in \mathbb{R}^{d \times C}$. Image-text alignment is optimized based on the cosine similarity of features.

During the testing phase, CLIP is capable of classifying a query image x into C possible categories. This is accomplished by computing the cosine similarity between the query image embedding vector and the set of text embeddings W . The prediction probability is then determined using the formula:

$$p(y|z) = \frac{\exp(\text{sim}(z, W_y)/\tau)}{\sum_{i=1}^C \exp(\text{sim}(z, W_i)/\tau)}, \quad (1)$$

where $\text{sim}(\cdot, \cdot)$ denotes the cosine similarity, and τ is a learned temperature parameter.

3.2. Revisiting Previous Efficient Transfer Paradigms

Motivated by the effectiveness of Efficient Transfer Learning (ETL) techniques in natural language processing, such as prompt tuning and Adapter, recent developments like CoCoOp and CLIP-Adapter have adapted these concepts for use in visual-language models (VLMs).

CoOp [30] introduces prompt tuning to VLMs for the first time, utilizing M learnable context vectors $v = \{v_1, v_2, \dots, v_M\}$ to generate task-specific templates, replacing the fixed text prompt templates used in CLIP. Specifically, $t_i = \{v_1, v_2, \dots, v_M, c_i\}$ integrates learnable context vectors v with the class token embedding c_i . This combined prompt is then input into the text encoder $g(\cdot)$. During training process, CoOp maintains the pre-trained VLMs parameters unchanged and solely adjusts the learnable vectors v . CoCoOp [29] is an enhanced version of CoOp. CoOp suggests that contexts conditioned on individual instances offer superior generalization because they pivot attention from a narrow set of classes (thus reducing overfitting risks) toward each unique input instance, facilitating broader task applicability. Meanwhile, CoCoOp introduces a Meta-Net to produce a conditional token that is subsequently amalgamated with the context vectors, enhancing adaptability and specificity to each instance.

Adapter-style tuning integrates extra modules $\phi_\omega(\cdot)$ into pre-trained models to modify the pre-trained features f into new features f' . Generally, adapter-style tuning can be expressed as:

$$f' = f + \alpha \phi_\omega(f) \quad (2)$$

where α is a scaling factor. In CLIP-Adapter, the adapter module ϕ_ω consists of two linear transformation layers with

a ReLU activation function situated between them. CLIP-Adapter explores the use of adapters for both visual and textual components, applying the adapter module separately to the image and text branches of CLIP. This investigation reveals that both types of adapters—visual and textual—yield similarly effective performance. When training on downstream tasks, adapter-style approaches like CLIP-Adapter focus on tuning the parameters of these adapter modules only, leaving the foundational pre-trained CLIP model parameters unchanged. This strategy allows for task-specific customization while maintaining the general capabilities of the underlying model. Moreover, recent developments in SuS-X [23] and C2A [21] have utilized generative diffusion models or large-scale external databases to achieve enhanced feature representations f' .

4. Approach

In this section, we will provide a detailed description of the two prototype rectification strategies, i.e., conditional adapter and nearest neighbor rectification. The whole framework of our conditional prototype rectification prompt learning is depicted in Figure 4, which is composed of two strategy, including conditional adapter and nearest neighbor rectification.

4.1. Conditional Adapter

Previous works like CoCoOp [29] considered how input images impact text prototypes. And CLIP-Adapter [9], TaskRes [27], and Tip-Adapter [28] derive features using separate visual or textual features. In contrast, we propose conditional adapter (CoAdapter), which leverages the connections between input images and both visual and textual prototypes, modeling sample-specific knowledge for downstream tasks through the integrated textual and visual structural knowledge.

As shown in Figure 4 (a), the conditional adapter is developed based on CoOp [30]. For a given input image x , we utilize the feature z of the input image and the relationship between the image prototype \mathbf{V} /text prototype \mathbf{W} to generate a sample-specific residual. This entails processing both the feature z and the prototypes through a transformer block, which then produces the sample-specific residual. Specifically, we apply the image feature as query and the prototype embeddings as both key and value into an attention block. Then, the visual residual $R_v \in \mathbb{R}^{d \times C}$ is calculated as an exemplar of the sample-specific residual using the following set of equations:

$$Q_v, K_v, V_v = F_q(z), F_k(\mathbf{V}), F_v(\mathbf{V}), \quad (3)$$

$$R_v = \text{Norm}(\text{FFN}_0(\text{Softmax}(\frac{Q_v \cdot K_v^\top}{\sqrt{d}})V_v) + \text{FFN}_1(x)), \quad (4)$$

where Norm denotes the layer normalization process. The F_q , F_k and F_v represent the multilayer perceptron layers that generate the query, key, and value for the attention mechanism, respectively. The terms FFN_0 and FFN_1 are also multilayer perceptrons involved in further processing the attention output and the original input feature z before combining them. By using a similar computation method to visual residuals, we can obtain the textual residual R_t . Afterward, the fused features $P = \mathbf{W} + R_t + R_v$ are aggregated and used as refined textual prototype for classification, effectively combining insights from both the visual and textual domains to improve the performance on specific tasks.

4.2. Nearest Neighbor Rectification

Inspired by C2A [21] and SuS-X [23] which enhance prototypes using generative diffusion models [3, 4, 20] or expansive external databases, our work seeks to enrich the limited knowledge obtained from few-shot samples. We aim to leverage the potential of unlabeled samples, circumventing the need for auxiliary or synthetic data, to mitigate the inherent biases and constraints associated with few-shot learning scenarios.

Due to data scarcity, the features P we derive might display considerable bias. To address this, we employ features extracted from high-confidence unlabeled images, which are utilized to refine and adjust the feature representation P , enhancing its robustness and generalizability. Specifically, for each class prototype P_i , we find its k nearest neighbors within the unlabeled dataset and utilize their features to recalibrate P_i . This adjustment process can be mathematically articulated as follows:

$$P'_i = \alpha \cdot P_i + (1 - \alpha) \cdot \frac{\sum_{j=1}^k z_j^u}{k}, \quad (5)$$

where z_j^u is the j -th nearest neighbor of the K nearest neighbors, and α is the hyper-parameter to adjust the weights of P and knowledge from unlabeled samples.

4.3. Tuning for Downstream Tasks

To ensure that the fused features P we obtain do not significantly deviate from those generated by the pre-trained CLIP model, and to enhance the generalizability of model, we employ a consistency constraint. This constraint encourages the fused features to remain similar to the representations from the original pre-trained model, which has learned robust and generalizable features from a vast amount of data. We use a pre-trained large language model (LLM) to generate more descriptive sentences from template textual inputs, which are then used to guide the fused features. By doing so, we ensure that the fused features have a high degree of similarity with the textually-augmented representations provided by the LLM. We can denote the consistency

constraint as:

$$\mathcal{L}_{cons} = \frac{1}{C} \sum_{i=1}^C \left(1 - \frac{P_i \cdot g(t_i)}{\|P_i\| \cdot \|g(t_i)\|}\right) \quad (6)$$

During training, we only update the learnable context vectors v together with the transformer block in CoAdapter, maintaining the base classifier and the image branch of CLIP unchanged. Given an image, supervised classification loss is computed as:

$$\mathcal{L}_{cls} = -\log \frac{\exp(\text{sim}(z, P'_y)/\tau)}{\sum_{i=1}^C \exp(\text{sim}(z, P'_i)/\tau)}. \quad (7)$$

Adding both losses with a balancing factor λ , we get the final loss function of CPR is:

$$\mathcal{L} = \mathcal{L}_{cls} + \lambda \cdot \mathcal{L}_{cons}. \quad (8)$$

5. Experiment

5.1. Datasets and Implementation Details

Similar to CoCoOp [29] and ProGrad [31], our evaluation of the proposed method encompasses two primary settings: 1) generalization from base to new classes within a dataset; and 2) few-shot image classification. These evaluations are conducted leveraging the pretrained CLIP [19] model, ensuring a consistent basis for comparison and thorough assessment of generalization and adaptability capabilities. More detailed results will be given in the Supplementary materials.

Datasets. Following CLIP [19], CoOp [30], CoCoOp [29], and ProGrad [31], the base-to-new generalization and few-shot image classification are conducted on 11 image classification datasets, i.e., ImageNet [6] and Caltech101 [8] for generic object classification; OxfordPets [18], StanfordCars [14], Flowers102 [17], Food101 [2], and FGVCIAircraft [16] for fine-grained visual categorization, EuroSAT [11] for satellite image classification, UCF101 [22] for action recognition, DTD [5] for texture classification, and SUN397 [25] for scene recognition.

Training details. Our experiments are executed using the same frameworks as established in CoOp [30] and ProGrad [31], incorporating the CLIP model as the core component. The experiments utilize ResNet-50 [10] and ViT-B/16 [7] as vision backbones, aligning with the setups in CoOp where the context length is consistently held at 16. To ensure statistical reliability and fairness in comparison, the reported performance metrics are the averages derived from three distinct random seeds. Consistency with the original studies also extends to the training scheme; we adhere to the same training epochs, training schedule, and data augmentation strategies as described in CoOp [30] and ProGrad [31]. Regarding hyperparameters, we set the α for the

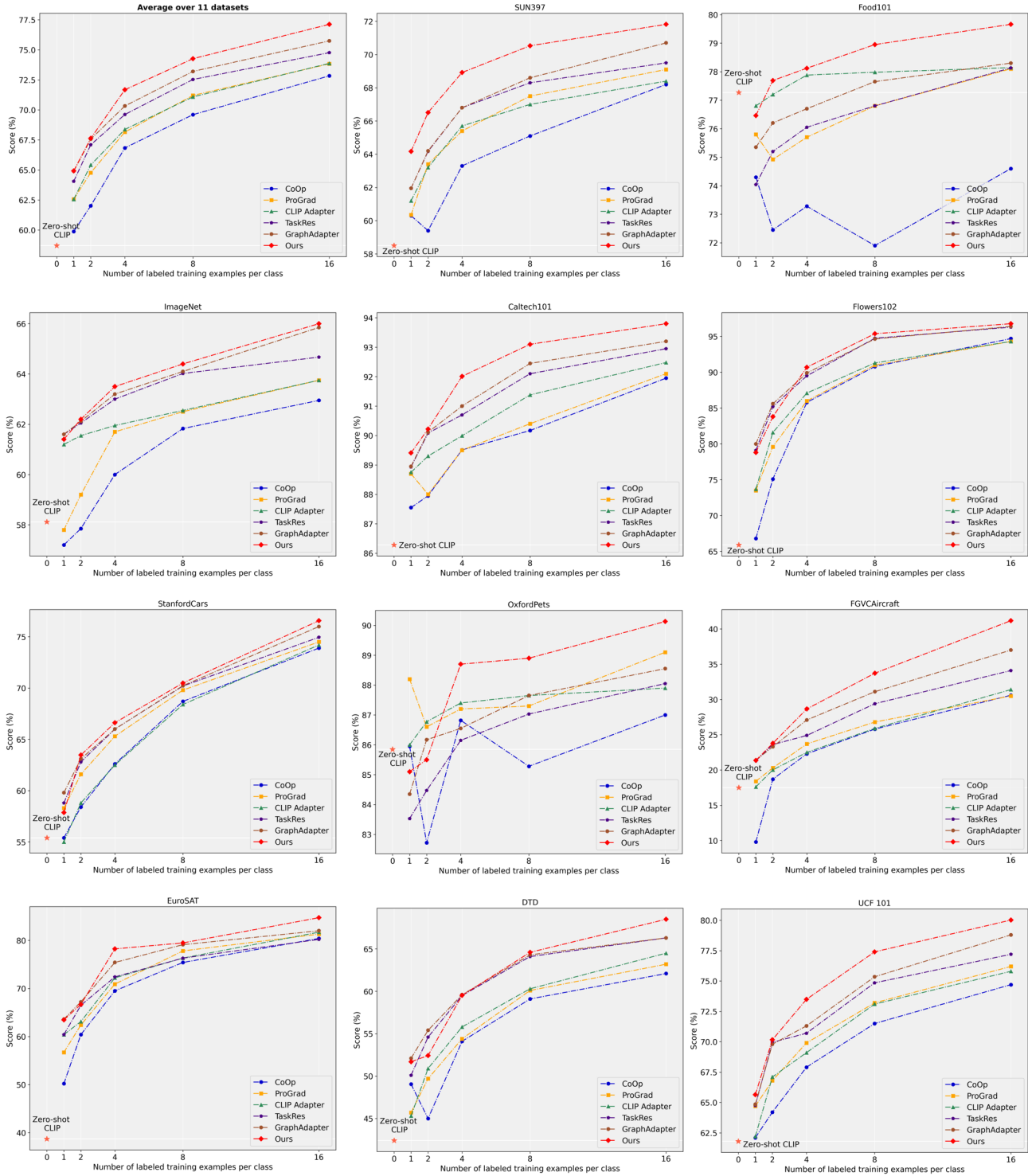


Figure 3. The performance comparison for few-shot learning (1-/2-/4-/8-/16-shot) is conducted on 11 benchmark datasets, with the top-left indicating the averaged accuracy across these datasets.

base-to-new generalization and the few-shot learning setups to 8.0 and 1.0, respectively, and uniformly set alpha (α) to

0.95, and we adjust the number of neighbors (k) to 5. The computational groundwork for all experiments is provided

Table 1. Comparison with existing methods in the base-to-new generalization setting with ViT-B/16 as the backbone. The context length M is 4 for prompt-based methods with the 16-shots samples from the base classes. H: Harmonic mean.

| (a) Average over 11 datasets | | | | (b) ImageNet | | | | (c) Caltech101 | | | |
|------------------------------|--------------|--------------|--------------|------------------|--------------|--------------|--------------|----------------|--------------|--------------|--------------|
| | Base | New | H | | Base | New | H | | Base | New | H |
| CLIP | 69.34 | 74.22 | 71.70 | CLIP | 72.43 | 68.14 | 70.22 | CLIP | 96.84 | 94.00 | 95.40 |
| CoOp | 82.63 | 67.99 | 74.60 | CoOp | 76.46 | 66.31 | 71.02 | CoOp | 98.11 | 93.52 | 95.76 |
| CoCoOp | 80.47 | 71.69 | 75.83 | CoCoOp | 75.98 | 70.43 | 73.10 | CoCoOp | 97.96 | 93.81 | 95.84 |
| ProGrad | 82.48 | 70.75 | 76.16 | ProGrad | 77.02 | 66.66 | 71.46 | ProGrad | 98.02 | 93.89 | 95.91 |
| KgCoOp | 80.73 | 73.60 | 77.00 | KgCoOp | 75.83 | 69.96 | 72.78 | KgCoOp | 97.72 | 94.39 | 96.03 |
| MaPLe | 82.28 | 75.14 | 78.55 | MaPLe | 76.66 | 70.54 | 73.47 | MaPLe | 97.74 | 94.36 | 96.02 |
| CPR | 83.81 | 76.21 | 79.82 | CPR | 77.21 | 70.60 | 73.75 | CPR | 98.64 | 95.41 | 97.00 |
| (d) OxfordPets | | | | (e) StanfordCars | | | | (f) Flowers102 | | | |
| | Base | New | H | | Base | New | H | | Base | New | H |
| CLIP | 91.17 | 97.26 | 94.12 | CLIP | 63.37 | 74.89 | 68.65 | CLIP | 72.08 | 77.80 | 74.83 |
| CoOp | 94.24 | 96.66 | 95.43 | CoOp | 76.20 | 69.14 | 72.49 | CoOp | 97.63 | 69.55 | 81.23 |
| CoCoOp | 95.20 | 97.69 | 96.43 | CoCoOp | 70.49 | 73.59 | 72.01 | CoCoOp | 94.87 | 71.75 | 81.71 |
| ProGrad | 95.07 | 97.63 | 96.33 | ProGrad | 77.68 | 68.63 | 72.88 | ProGrad | 95.54 | 71.87 | 82.03 |
| KgCoOp | 94.65 | 97.76 | 96.18 | KgCoOp | 71.76 | 75.04 | 73.36 | KgCoOp | 95.00 | 74.73 | 83.65 |
| MaPLe | 95.43 | 97.76 | 96.58 | MaPLe | 72.94 | 74.00 | 73.47 | MaPLe | 95.92 | 72.46 | 82.56 |
| CPR | 95.48 | 97.77 | 96.61 | CPR | 77.39 | 75.12 | 76.24 | CPR | 96.96 | 79.08 | 87.11 |
| (g) Food101 | | | | (h) FGVCAircraft | | | | (i) SUN397 | | | |
| | Base | New | H | | Base | New | H | | Base | New | H |
| CLIP | 90.10 | 91.22 | 90.66 | CLIP | 27.19 | 36.29 | 31.09 | CLIP | 69.36 | 75.35 | 72.23 |
| CoOp | 89.44 | 87.50 | 88.46 | CoOp | 39.24 | 30.49 | 34.30 | CoOp | 80.85 | 68.34 | 74.07 |
| CoCoOp | 90.70 | 91.29 | 90.99 | CoCoOp | 33.41 | 23.71 | 27.74 | CoCoOp | 79.74 | 76.86 | 78.27 |
| ProGrad | 90.37 | 89.59 | 89.98 | ProGrad | 40.54 | 27.57 | 32.82 | ProGrad | 81.26 | 74.17 | 77.55 |
| KgCoOp | 90.50 | 91.70 | 91.09 | KgCoOp | 36.21 | 33.55 | 34.83 | KgCoOp | 80.29 | 76.53 | 78.36 |
| MaPLe | 90.71 | 92.05 | 91.38 | MaPLe | 37.44 | 35.61 | 36.50 | MaPLe | 80.82 | 78.70 | 79.75 |
| CPR | 90.95 | 92.03 | 91.48 | CPR | 41.00 | 35.69 | 38.16 | CPR | 82.38 | 79.44 | 80.89 |
| (j) DTD | | | | (k) EuroSAT | | | | (l) UCF101 | | | |
| | Base | New | H | | Base | New | H | | Base | New | H |
| CLIP | 53.24 | 59.90 | 56.37 | CLIP | 56.48 | 64.05 | 60.03 | CLIP | 70.53 | 77.50 | 73.85 |
| CoOp | 80.17 | 47.54 | 59.68 | CoOp | 91.54 | 54.44 | 68.27 | CoOp | 85.14 | 64.47 | 73.37 |
| CoCoOp | 77.01 | 56.00 | 64.85 | CoCoOp | 87.49 | 60.04 | 71.21 | CoCoOp | 82.33 | 73.45 | 77.64 |
| ProGrad | 77.35 | 52.35 | 62.45 | ProGrad | 90.11 | 60.89 | 72.67 | ProGrad | 84.33 | 74.94 | 79.35 |
| KgCoOp | 77.55 | 54.99 | 64.35 | KgCoOp | 85.64 | 64.34 | 73.48 | KgCoOp | 82.89 | 76.67 | 79.65 |
| MaPLe | 80.36 | 59.18 | 68.16 | MaPLe | 94.07 | 73.23 | 82.35 | MaPLe | 83.00 | 78.66 | 80.77 |
| CPR | 82.87 | 58.45 | 68.55 | CPR | 92.71 | 74.18 | 82.41 | CPR | 86.35 | 79.83 | 82.96 |

by NVIDIA RTX A100 80G GPUs, ensuring robust and efficient processing capabilities for our analyses.

Baselines. Four type of CoOp-based methods and three adapter-style methods are treated as baselines for com-

parison: CoOp [30], CoCoOp [29], ProGrad [31], KgCoOp [26], MaPLe [13], CLIP-Adapter [9], TaskRes [27] and GraphAdapter [15].

| Metric | Baseline | w/o CoAdapter | w/o NNR | w/o \mathcal{L}_{cons} | CPR |
|--------|----------|---------------|---------|--------------------------|--------------|
| Base | 82.63 | 83.13 | 83.04 | 83.09 | 83.81 |
| New | 67.99 | 71.99 | 71.74 | 73.18 | 76.21 |
| H | 74.60 | 76.71 | 76.52 | 77.52 | 79.82 |

Table 2. Ablation studies.

| Model | 1-shot | 2-shot | 4-shot | 8-shot | 16-shot |
|-------------|--------------|--------------|--------------|--------------|--------------|
| CoAdapter-I | 16.55 | 20.76 | 24.04 | 28.23 | 32.34 |
| CoAdapter-T | 19.92 | 22.23 | 24.72 | 28.26 | 32.10 |
| CoAdapter | 21.36 | 23.79 | 28.66 | 33.72 | 41.17 |

Table 3. Performance comparison of three CoAdapter variants on FGVCaircraft under few-shot learning setting.

5.2. Few-shot Classification

The results of our experiments are illustrated in Figure 3, demonstrating the superior performance of our CPR method relative to previous ETL approaches across varying shot evaluations (1-/2-/4-/8-/16-shot) when averaged over 11 benchmark datasets. In particular, during the 16-shot evaluation, CPR attains an average success rate of 77.12%, surpassing GraphAdapter by 1.38% and TaskRes by 2.37%. It is worth noting that CPR maintains its lead in performance even in the demanding FGVCaircraft dataset, which focuses on fine-grained classification, outstripping GraphAdapter by 4.17% in the 16-shot setting. Our CPR can achieve these promising results because CPR can alleviate overfitting by exploiting the structure knowledge with the dual prototypes and using knowledge from unlabeled data.

5.3. Generalization From Base-to-New Classes

Similar to previous works [13, 26, 29–31], we divide each dataset into two categories: base classes (Base) and new classes (New). Mirroring the zero-shot setting, the new classes are disjoint from the base classes. To assess the generalizability of the CoOp-based approaches, all evaluated methods, including the proposed CPR, utilize the base classes for tuning and perform evaluations on the new classes. The specific results are detailed in Table 1, which provides comprehensive performance metrics across all 11 datasets using the ViT-B/16 backbone with 16-shot samples.

As shown in Table 1, CPR method surpasses existing methodologies in achieving a higher average performance based on the Harmonic mean across all settings, underlining its enhanced capability for generalizing from base to new classes. Specifically, CPR demonstrates superior performance on new classes in nine out of the eleven datasets, including ImageNet, Caltech101, OxfordPets, StanfordCars, Flowers102, FGVCaircraft, SUN397, EuroSAT, and

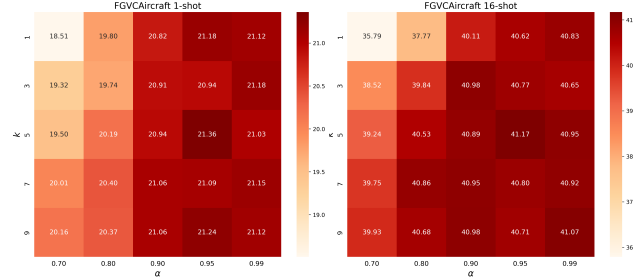


Figure 4. The ablation studies for two coefficients α and k on FGVCaircraft under few-shot learning setting.

UCF101. The exceptional performance highlights the improvement of CPR in generalization to new classes compared to the current methods. Moreover, CPR consistently achieves top results for the base classes in the majority of scenarios. Hence, CPR effectively enhances generalizability to new classes while maintaining or even improving base class performance, thereby securing the highest Harmonic mean across all evaluated datasets.

5.4. Ablation Studies

The effects of each prototype rectification strategy in CPR. To evaluate the effectiveness of the proposed strategy, ablation studies were conducted. As shown in Table 2, the results indicate that both strategies significantly enhanced the generalizability of model and mitigated overfitting relative to the base class. If the CoAdapter is removed from CPR, the accuracy on new class recognition tasks would decrease by 5.5%. Similarly, if NNR is not used, the accuracy would decrease by 5.9%. These research findings confirm that each strategy can independently enhance recognition performance, and their synergistic application is particularly effective in improving accuracy in efficient transfer learning scenarios.

The effects of dual prototype in CoAdapter. The distinctiveness of our CoAdapter lies in its utilization of dual prototypes to generate sample-conditioned text tokens. Therefore, we investigate the effectiveness of another two variants of our GraphAdapter, i.e., CoAdapter-I, and CoAdapter-T. CoAdapter-I leverages only the visual prototype for generating sample-conditioned text tokens, whereas CoAdapter-T employs solely the textual prototype for this purpose. As shown in Table 3, the CoAdapter exhibits superior performance when it simultaneously leverages the prototypes from both modalities. This enhancement can be attributed to the complementary nature of the information provided by each modality: the visual modality offers details about object appearance and structure, while the textual modality provides semantic and contextual insights. The integration of these diverse information streams enables the CoAdapter to develop more comprehensive and robust data representa-

| Backbone | Model | Base | New | H |
|------------|-------|--------------|--------------|--------------|
| ResNet-50 | CoOp | 27.01 | 24.48 | 25.68 |
| | CPR | 28.21 | 26.51 | 27.34 |
| ResNet-101 | CoOp | 31.75 | 25.97 | 28.57 |
| | CPR | 33.07 | 29.27 | 31.06 |
| ViT-B/32 | CoOp | 30.49 | 25.67 | 27.88 |
| | CPR | 30.85 | 29.45 | 30.14 |
| ViT-B/16 | CoOp | 39.24 | 30.49 | 34.30 |
| | CPR | 41.00 | 35.69 | 38.16 |

Table 4. Comparisons different backbones on FGVCaircraft under base-to-new generalization setting.

tions, thereby improving its generalization capabilities and performance on downstream tasks.

The effects of neighbors in NNR. In the Nearest Neighbor Rectification (NNR) strategy, determining the optimal value of k —the number of nearest unlabeled samples to associate with each fused prototype P_i —is essential for knowledge completion across each class. To ascertain the most appropriate k value, we conducted an ablation study within a few-shot learning framework, evaluating k values from the set 1, 3, 5, 7, 9. The results, depicted in Figure 4, reveal that the model attains its best performance when k is set to 5. This outcome implies that, within the context of our experiments, integrating information from five nearest neighbors achieves the optimal balance between acquiring sufficient knowledge and mitigating the influence of irrelevant information, thereby enhancing the predictive accuracy of model most effectively.

The effects of α in NNR. In the Nearest Neighbor Rebalancing (NNR) strategy, the parameter α plays a pivotal role in determining the extent to which the model benefits from the knowledge in unlabeled data. To identify the ideal setting for α , we carried out a series of ablation experiments. As shown in Figure 4, the results indicate that the model achieves optimal performance when α is set to 0.95. This outcome suggests that an appropriate α value can effectively balance the insights from unlabeled data with the requirements to ensure the reliability of the correction process. In contrast, too high of an α value might not fully utilize the embedded knowledge in the unlabeled data, while too low of an α might introduce unnecessary noise or irrelevant details, potentially impairing the performance.

The effects of different backbones. As shown in Table 4, we also evaluate the effectiveness of our Conditional Prototype Rectification Prompt Learning (CPR) method across various CLIP visual backbones, namely ResNet-50, ResNet-101, ViT-B/32, and ViT-B/16. Across all four visual backbones, CPR consistently outperforms prior methods, demonstrating its robustness and adaptability to differ-

| λ | Base-to-New | | | Few-shot Learning | | | | |
|-----------|--------------|--------------|--------------|-------------------|--------------|--------------|--------------|--------------|
| | Base | New | H | 1-shot | 2-shot | 4-shot | 8-shot | 16-shot |
| 0.0 | 38.78 | 34.83 | 36.69 | 19.11 | 22.38 | 26.79 | 32.85 | 41.03 |
| 0.1 | 39.02 | 34.01 | 36.34 | 19.25 | 23.32 | 27.65 | 33.65 | 40.97 |
| 1.0 | 42.80 | 33.95 | 37.87 | 21.36 | 23.79 | 28.66 | 33.72 | 41.17 |
| 2.0 | 41.18 | 32.03 | 36.03 | 21.05 | 23.12 | 28.42 | 33.22 | 40.86 |
| 5.0 | 40.88 | 35.33 | 37.90 | 20.88 | 22.99 | 27.97 | 33.12 | 40.54 |
| 8.0 | 41.00 | 35.69 | 38.16 | 20.99 | 22.76 | 27.88 | 33.21 | 40.76 |
| 10.0 | 39.44 | 35.31 | 37.26 | 20.64 | 22.54 | 27.75 | 333.04 | 40.74 |

Table 5. The ablation studies for coefficient λ on FGVCaircraft.

ent underlying architectures. This result highlights versatility of CPR and its ability to leverage distinct visual features extracted by various backbones, thus affirming its broad applicability and effectiveness in enhancing model performance.

The effects of λ . To investigate the effectiveness of hyperparameter λ , as specified in Equation (8) in Section 4.3, we conduct experiments on FGVCaircraft by varying different λ . \mathcal{L}_{cons} aims to enhance the generalizability for unseen classes by minimizing the distance between learnable fused features and fixed textual enhanced representations provided by the LLM As shown in Table 4, selecting an optimal value for λ is crucial for enhancing model performance. Specifically, for base-to-new generalization, setting λ to 8 yields the most beneficial outcome. An appropriate λ can avoid learning text tokens with poor generalization on base classes while generating sample-specific representations. On the other hand, for few-shot learning setting, the optimal performance is observed when λ is adjusted to 1.

Limitations. The limitation of our CPR is rooted in the selection process of unlabeled data. In our current methodology, we employ a k -nearest neighbor algorithm to identify supplementary knowledge. While this strategy provides a foundational approach to augmenting our dataset, it lacks a definitive level of confidence, potentially limiting the quality of the knowledge integration. We posit that a more precise and sophisticated selection method could significantly enhance the quality of the supplementary knowledge, thereby improving the performance on downstream tasks.

6. Conclusion

In this paper, we provide an in-depth examination of the constraints faced by previous approaches in scenarios characterized by scarce data, identifying two main limitations: 1) the reliance on a single modality for modeling task-specific knowledge, and 2) the employment of resource-intensive and protracted techniques for knowledge enhancement, which are crucial for tasks requiring data efficiency. To address these issues, we introduce an innovative Conditional Prototype Rectification Prompt Learning (CPR) methodology for visual-language models. CPR aims to rectify biases present in base exam-

ples and effectively enrich limited datasets. It achieves this by amalgamating fused textual and visual prototype knowledge with insights gleaned from unlabeled samples, thereby enabling the classifier to adapt more effectively to downstream tasks. Our comprehensive testing across 11 benchmark datasets demonstrates the effectiveness of our CPR on few-shot learning and generalization.

References

- [1] Jean-Baptiste Alayrac, Jeff Donahue, Pauline Luc, Antoine Miech, Iain Barr, Yana Hasson, Karel Lenc, Arthur Mensch, Katherine Millican, Malcolm Reynolds, Roman Ring, Eliza Rutherford, Serkan Cabi, Tengda Han, Zhitao Gong, Sina Samangooei, Marianne Monteiro, Jacob L. Menick, Sebastian Borgeaud, Andy Brock, Aida Nematzadeh, Sahand Sharifzadeh, Mikolaj Binkowski, Ricardo Barreira, Oriol Vinyals, Andrew Zisserman, and Karén Simonyan. Flamingo: a visual language model for few-shot learning. In *NeurIPS*, 2022. 1
- [2] Lukas Bossard, Matthieu Guillaumin, and Luc Van Gool. Food-101—mining discriminative components with random forests. In *ECCV*, pages 446–461, 2014. 5
- [3] Tim Brooks, Aleksander Holynski, and Alexei A Efros. Instructpix2pix: Learning to follow image editing instructions. In *CVPR*, 2023. 5
- [4] Haoxing Chen, Zhuoer Xu, Zhangxuan Gu, Jun Lan, Xing Zheng, Yaohui Li, Changhua Meng, Huijia Zhu, and Weiqiang Wang. Diffute: Universal text editing diffusion model. In *NeurIPS*, 2023. 5
- [5] Mircea Cimpoi, Subhransu Maji, Iasonas Kokkinos, Sammy Mohamed, and Andrea Vedaldi. Describing textures in the wild. In *CVPR*, pages 3606–3613, 2014. 5
- [6] Jia Deng, Wei Dong, Richard Socher, Li-Jia Li, Kai Li, and Li Fei-Fei. Imagenet: A large-scale hierarchical image database. In *CVPR*, pages 248–255, 2009. 5
- [7] Alexey Dosovitskiy, Lucas Beyer, Alexander Kolesnikov, Dirk Weissenborn, Xiaohua Zhai, Thomas Unterthiner, Mostafa Dehghani, Matthias Minderer, Georg Heigold, Sylvain Gelly, Jakob Uszkoreit, and Neil Houlsby. An image is worth 16x16 words: Transformers for image recognition at scale. In *ICLR*, 2021. 3, 5
- [8] Li Fei-Fei, Robert Fergus, and Pietro Perona. Learning generative visual models from few training examples: An incremental bayesian approach tested on 101 object categories. *Comput. Vis. Image Underst.*, 106(1):59–70, 2007. 5
- [9] Peng Gao, Shijie Geng, Renrui Zhang, Teli Ma, Rongyao Fang, Yongfeng Zhang, Hongsheng Li, and Yu Qiao. Clip-adapter: Better vision-language models with feature adapters. *IJCV*, pages 1–15, 2023. 1, 2, 4, 7
- [10] Kaiming He, Xiangyu Zhang, Shaoqing Ren, and Jian Sun. Deep residual learning for image recognition. In *CVPR*, pages 770–778, 2016. 3, 5
- [11] Patrick Helber, Benjamin Bischke, Andreas Dengel, and Damian Borth. Eurosat: A novel dataset and deep learning benchmark for land use and land cover classification. *J-STARS*, 12(7):2217–2226, 2019. 5
- [12] Chao Jia, Yinfei Yang, Ye Xia, Yi-Ting Chen, Zarana Parekh, Hieu Pham, Quoc V. Le, Yun-Hsuan Sung, Zhen Li, and Tom Duerig. Scaling up visual and vision-language representation learning with noisy text supervision. In *ICML*, pages 4904–4916, 2021. 1
- [13] Muhammad Uzair Khattak, Hanoona Abdul Rasheed, Muhammad Maaz, Salman H. Khan, and Fahad Shahbaz Khan. Maple: Multi-modal prompt learning. In *CVPR*, pages 19113–19122, 2023. 7, 8
- [14] Jonathan Krause, Michael Stark, Jia Deng, and Li Fei-Fei. 3d object representations for fine-grained categorization. In *ICCV Workshop*, pages 554–561, 2013. 5
- [15] Xin Li, Dongze Lian, Zhihe Lu, Jiawang Bai, Zhibo Chen, and Xinchao Wang. Graphadapter: Tuning vision-language models with dual knowledge graph. In *NeurIPS*, 2023. 1, 7
- [16] Subhransu Maji, Esa Rahtu, Juho Kannala, Matthew Blaschko, and Andrea Vedaldi. Fine-grained visual classification of aircraft. *arXiv preprint arXiv:1306.5151*, 2013. 5
- [17] Maria-Elena Nilsback and Andrew Zisserman. Automated flower classification over a large number of classes. In *ICVGIP*, pages 722–729, 2008. 5
- [18] Omkar M. Parkhi, Andrea Vedaldi, Andrew Zisserman, and C. V. Jawahar. Cats and dogs. In *CVPR*, pages 3498–3505, 2012. 5
- [19] Alec Radford, Jong Wook Kim, Chris Hallacy, Aditya Ramesh, Gabriel Goh, Sandhini Agarwal, Girish Sastry, Amanda Askell, Pamela Mishkin, Jack Clark, et al. Learning transferable visual models from natural language supervision. In *ICML*, pages 8748–8763, 2021. 1, 3, 5
- [20] Robin Rombach, Andreas Blattmann, Dominik Lorenz, Patrick Esser, and Björn Ommer. High-resolution image synthesis with latent diffusion models. In *CVPR*, pages 10684–10695, 2022. 5
- [21] Aniket Roy, Anshul Shah, Ketul Shah, Anirban Roy, and Rama Chellappa. Cap2aug: Caption guided image to image data augmentation. *arXiv preprint arXiv:2212.05404v2*, 2023. 2, 4, 5
- [22] Khurram Soomro, Amir Roshan Zamir, and Mubarak Shah. Ucf101: A dataset of 101 human actions classes from videos in the wild. *arXiv preprint arXiv:1212.0402*, 2012. 5
- [23] Vishaal Udandarao, Ankush Gupta, and Samuel Albanie. Sus-x: Training-free name-only transfer of vision-language models. In *ICCV*, pages 2725–2736, 2023. 2, 4, 5
- [24] Ashish Vaswani, Noam Shazeer, Niki Parmar, Jakob Uszkoreit, Llion Jones, Aidan N. Gomez, Lukasz Kaiser, and Illia Polosukhin. Attention is all you need. In *NeurIPS*, pages 5998–6008, 2017. 3
- [25] Jianxiong Xiao, James Hays, Krista A Ehinger, Aude Oliva, and Antonio Torralba. Sun database: Large-scale scene recognition from abbey to zoo. In *CVPR*, pages 3485–3492, 2010. 5
- [26] Hantao Yao, Rui Zhang, and Changsheng Xu. Visual-language prompt tuning with knowledge-guided context optimization. In *CVPR*, pages 6757–6767, 2023. 1, 7, 8
- [27] Tao Yu, Zhihe Lu, Xin Jin, Zhibo Chen, and Xinchao Wang. Task residual for tuning vision-language models. In *CVPR*, pages 10899–10909, 2023. 1, 2, 3, 4, 7

- [28] Renrui Zhang, Wei Zhang, Rongyao Fang, Peng Gao, Kun-chang Li, Jifeng Dai, Yu Qiao, and Hongsheng Li. Tip-adapter: Training-free adaption of clip for few-shot classification. In *ECCV*, pages 493–510, 2022. 4
- [29] Kaiyang Zhou, Jingkang Yang, Chen Change Loy, and Ziwei Liu. Conditional prompt learning for vision-language models. In *CVPR*, pages 16816–16825, 2022. 1, 4, 5, 7, 8
- [30] Kaiyang Zhou, Jingkang Yang, Chen Change Loy, and Ziwei Liu. Learning to prompt for vision-language models. *IJCV*, 130(9):2337–2348, 2022. 1, 4, 5, 7
- [31] Beier Zhu, Yulei Niu, Yucheng Han, Yue Wu, and Han-wang Zhang. Prompt-aligned gradient for prompt tuning. In *CVPR*, pages 15613–15623, 2023. 1, 5, 7, 8
- [32] Xiangyang Zhu, Renrui Zhang, Bowei He, Aojun Zhou, Dong Wang, Bin Zhao, and Peng Gao. Not all features matter: Enhancing few-shot clip with adaptive prior refinement. *arXiv preprint arXiv:2304.01195*, 2023. 1